Sea-ice Surface Temperature Retrieval and Validation for Copernicus Sentinel-3 Sea and Land Surface Temperature Radiometer - EUMETSAT ITT No. 215580

Review of state-of-the-art methods and algorithms for Ice Surface Temperature retrieval algorithms - Including consolidate and refine output product requirements and software specification

Document Reference Number: EUM/OPS-COPER/19/1065840

Authors:

Gorm Dybkjaer, Rasmus Tonboe, Mai Winstrup and Jacob Hoyer

Version 2.3

Requirement Baseline document

Deliverable 4 (D4)

The Danish Meteorological Institute

27-02-2020

Scope of this Report

The overall objective of this study is to develop a seamless sea-ice surface temperature (IST) and marginal ice zone temperature (MIZT) retrieval algorithm for the Copernicus Sentinel-3 Sea and Land Surface Temperature Radiometer (SLSTR).

The report contains a review of relevant scientific literature and other documentation of existing ice surface temperature products. This includes recommendations for the best suited algorithm or compound algorithm for IST and MIZT estimation from SLSTR data, based on surface emission and atmospheric transfer theory.

The report also discusses general requirements for the IST product and production, such as performance and IO requirements, uncertainty and quality level algorithms. Recommendations regarding in situ data sources for validation and discussions about algorithm calibration are also included.

The report is the baseline input to the WP 4 (algorithm development) and WP 5 (product generation).

Document Change Record.

Version	Date	Author	Description
v1.0	February 5th 2019	Gorm Dybkjaer	Requirement Baseline Document (D4)
V2.0	April 10th 2019	Gorm Dybkjaer	Response to RIDS
V2.1	May 1st 2019	Gorm Dybkjaer	Recommended algorithm summary in section 3.5.1 is added. Document reference number added.
V2.2	December 19th 2019	Jacob Hoyer	Minor updates
V2.3	February 28 2020	Gorm Dybkjaer	Response to RIDS (added text in section 4.1, 4.2 and included extra references, added a table in chapter 6)

Table of content

Acronyms and abbreviations

AASTI	Arctic and Antarctic Surface Temperatures from Infrared data, DMI data set
(A)ATSR	(Advanced) Along-Track Scanning Radiometer
ARM	Atmospheric Radiation Measurement (weather station)
ATBD	Algorithm Theoretical Basis Document
AVHRR	Advanced Very High Resolution Radiometer
AWS	Automatic Weather Station
CF	The conventions for Climate and Forecast metadata
CMEMS	Copernicus Marine Environment Monitoring Service
Copernicus	The European Union's Earth Observation Programme
ECMWF	European Centre for Medium-Range Weather Forecasts
ESA	European Space Agency
EUMETSAT	European Organization for the Exploitation of Meteorological Satellites
Felyx	Free, open source, software system for the analysis of large Earth Observation datasets
GDS	GHRSST Data Specification
GHRSST	The Group for High Resolution Sea Surface Temperature
ICE-ARC	Ice, Climate, Economics - Arctic Research on Change, EU FP7 project
IO	Input Output
IST	Ice Surface Temperature
ITT	Invitation To Tender
KO	Kick-Off
L2, L3, L4	Level-2, Level-3, Level-4
LST	Land Surface Temperature
Metop	Meteorological Operational (EUMETSAT)
MIZ	Marginal Ice Zone
MIZT	Marginal Ice Zone Temperature
MODIS	Moderate Resolution Imaging spectroradiometer
MRTD	Sentinel-3 Mission Requirements Traceability Document
MUDB	Match-Up Data Base
NASA	National Aeronautics and Space Administration
NEdT	Noise-Equivalent-change-in-Temperature
NWP	Numerical Weather Prediction
OSISAF	Ocean and Sea Ice Satellite Application Facility
OSI-205	OSISAF operational L2 IST product based on Metop AVHRR and VIIRS data
RB	Requirements baseline document
PDF	Probability Density Function
PROMICE	Programme for Monitoring of the Greenland Ice Sheet
QC	Quality Control
RTM	Radiative Transfer Model
RTTOV	Radiative Transfer for TOVS (TIROS Operational Vertical Sounder)
SLSTR	Sea and Land Surface Temperature Radiometer
SOW	Statement of Work
GSOW	Generic Statement of Work
SST	Sea Surface Temperature
ST	Surface Temperature
Tb	Brightness Temperature
TIR	Thermal InfraRed
TOA	Top Of Atmosphere
VIIRS	Visible Infrared Imaging Radiometer Suite

1 Introduction

Precise and accurate satellite Ice Surface Temperature (IST) measurements are essential for models and climate applications, where small changes in the surface temperature can change a sea ice regime from perennial sea ice to seasonal sea ice. It was shown that an increased energy flux of approximately 5 W/m2 is equivalent to a 1 K increase of ice surface temperature (Steffen et al., 1993), which again can change the ice state from Multi Year Ice (MYI) to First Year Ice (FYI) (Björk and Söderkvist, 2002). A monthly mean skin temperature difference map between modelled skin temperatures and observed skin temperatures from the AASTI data record for September 2007 reveals differences up to 10 K with large geographically variability (Figure 1). This indicates large potential for the applicability of satellite IST data in e.g. modelling, provided high precision and accuracy of the satellite data.

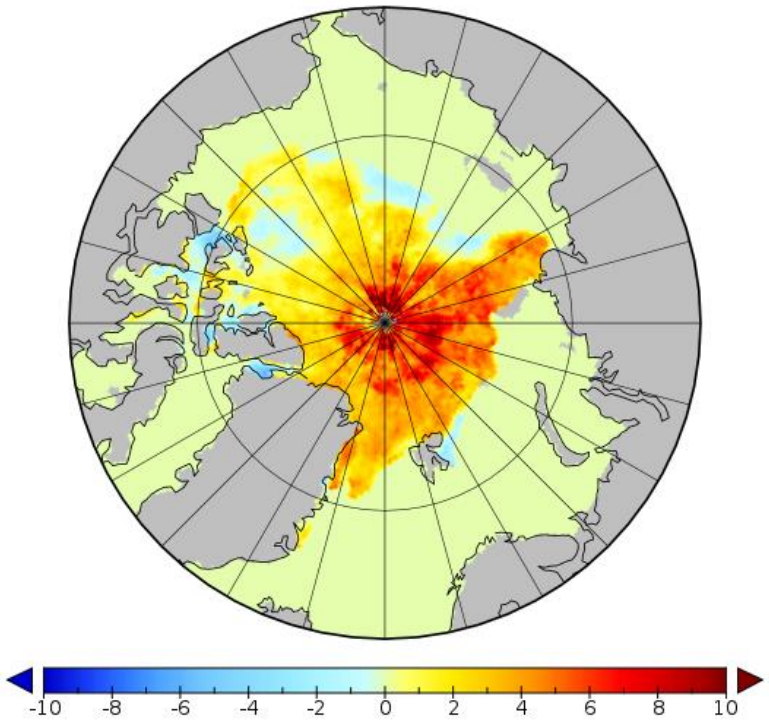

Figure 1: Mean temperature difference between modelled skin temperatures (NAOSIM) minus satellite observed skin temperatures (AASTI), September 2007.

However, determining the quality of satellite IST is not trivial, because in-situ IST observations from sea ice are typically sparse, and the fact that traditional observations may represent either temperatures from below the snow surface or air temperature, depending on the type of observation and the snow cover. In Figure 2, it is illustrated that bias and standard deviation between satellite IST and 1 meter and 2 meter temperatures (1mT and 2mT) and radiometric skin temperatures (Tskin) can be large. Bias was measured to 4.5 K and 1 K when comparing satellite IST to 2mT and Tskin observations, respectively. The figure also shows large differences in the error, when comparing satellite IST with in situ air and radiometric surface temperatures. Thorough quality control of in situ measurements is therefore important when it is used to estimate the performance of satellite IST algorithms.

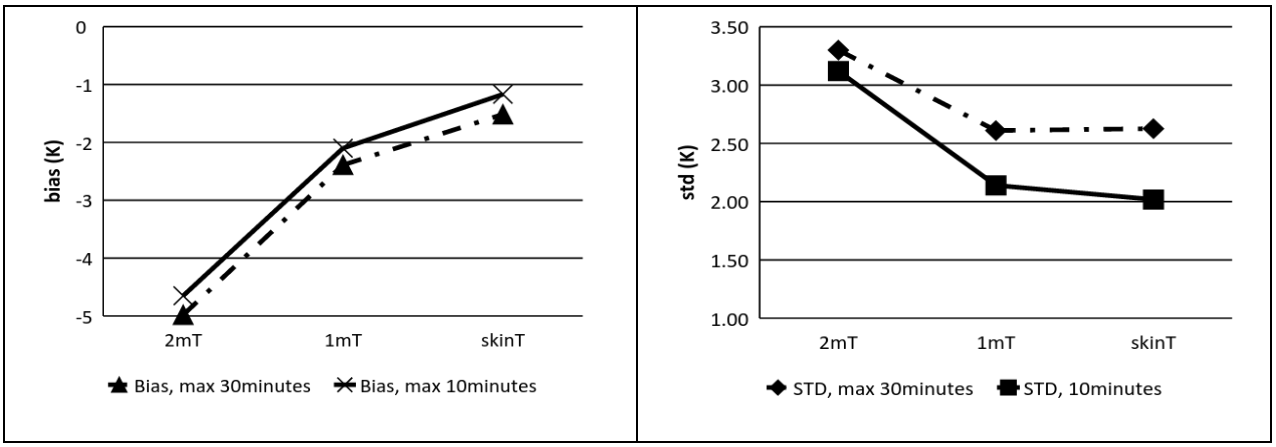

Figure 2 Metop IST compared with in situ airand skin temperature measurements: STD and bias from comparing Metop IST with 2m and 1m temperatures – within 10 min. (solid line) and 30 min. (dashed line). Data are recorded hourly between February 1 and June 1, 2016, on sea ice in Inglefield Bredning in NW Greenland, from a DMI AWS(ICE-ARC).

Several satellite IST products are available from Thermal InfraRed (TIR) sensors, all showing similar uncetainty statistics, typically around 2-4 K, depending on the validation context (Hoyer et al., 2017). With the SLSTR instrument we anticipate to create a satellite product with improved performance relative to existing satellite Thermal InfraRed (TIR) IST products, due to the advanced design of the SLSTR radiometers, and experience from the SLSTR predecessors, ATSR and AATSR (e.g. G.K. Corlett et al., 2006). We anticipate to lower the uncertainties in the retrieval algorithms themselves and the contribution from a low Noise Equivalent temperature difference (NEdT) and, finally, from the atmospheric properties due the high quality SLSTR radiometers.

It is important to note that the total uncertainty of the final SLSTR IST product is anticipated to be higher than the required 1 K mentioned in the project ITT and elsewhere (see chapter 4), because effects from insufficient cloud screening usually contribute with more than half of the total IST uncertainty (Dybkjaer et al. 2012, Hall et al. 2004b). Effects from non-detected clouds are particular large during darkness, where cloud detection is very difficult and faulty, due to missing information from the visible part of the spectrum. This is illustrated in Figure 3 where AVHRR IST (Dybkjaer et al., 2018) is compared with in situ IST using satellite based cloud screening versus cloud-screened based on down welling longwave radiation and air temperature relations (a good in situ estimation of cloud fraction). According to this comparison, undetected clouds contribute with approximately 2 K bias and raise the STD of differences from 1.6 K to 4.2 K.

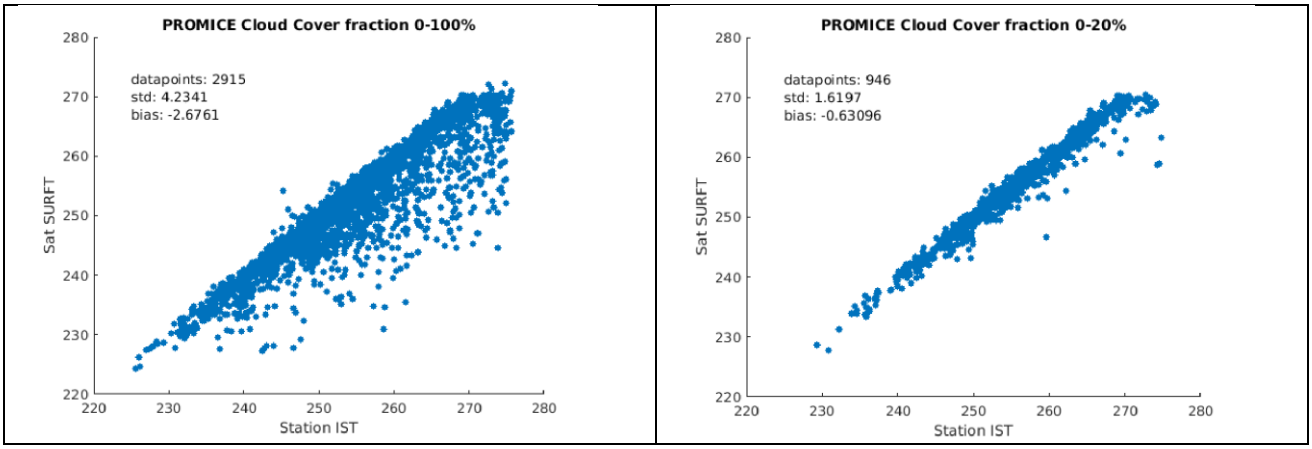

Figure 3 Satellite IST compared to all PROMICE surface temperature from the Greenland Ice Sheet using satellite cloud screening only (left panel) and ditto with the addition of an in-situ based cloud screening (right panel).

To obtain the best possible IST algorithm for the SLSTR instrument, we will test a range of algorithms using different constellations of SLSTR channels and view geometry, inspired by current LST and SST retrieval processors for SLSTR (Merchant, 2012), (Remedios and Emsley, 2012), and we will test the performance in different geographical and atmospheric regimes. The total uncertainty of the product will be deconstructed into basic components in an uncertainty algorithm, and each component will be evaluated and compared with existing uncertainty estimates.

2 Algorithms to be developed

Besides inspiration from earlier and current ST algorithms, the final choice of algorithm for the Sentinel-3 SLSTR IST processor will be based on various considerations and tests regarding snow surface and atmospheric properties in the Polar Regions. In addition, if time allows, we will test the feasibility of developing a new data-driven algorithm using machine-learning regression methods such as random forest and neural networks.

The following is a discussion of essential conditions that should be considered before selecting the best-suited algorithm. There is special focus on atmospheric correction, sampling, emissivity variability and calibration.

2.1 The dry polar atmosphere

Compared to temperate regions, the polar atmosphere is very dry, and several specialised algorithms have been developed for the retrieval of polar ice and sea surface temperatures using satellite infrared radiometry (Key and Haefliger, 1992; Stroeve et al., 1996; Vincent et al. 2008a). In temperate regions, the difference between the clear sky brightness temperatures measured at around 11 and 12 microns is primarily a function of water vapour in the atmosphere, and this relationship is exploited for atmospheric correction in split-window and two channel algorithms. However, in the dry polar atmosphere, the brightness temperature difference is typically not influenced by water vapour, and SST algorithms developed for temperate regions tend to overestimate SST in polar waters (Vincent et al., 2008a). Key and Haefliger (1992) found that the 11 and 12 microns channel difference over ice surfaces could be used for correcting snow surface emissivity variations instead of compensating for atmospheric water vapour. Stroeve et al. (1996) compared three different algorithms using ATSR data with surface radiometer measurements at the ETH-CU camp on the Greenland Ice Sheet. On the one hand, she found that using the dual view on the ATSR and two different channels (11 and 12 microns) performed much better than the split-window and the dual-view one-channel algorithms. Vincent et al. (2008a), on the other hand, found that single-channel and single-view algorithms performed much better than split-window algorithms in the North Water Polynya in Northern Baffin Bay. Both split window and single channel algorithms should be tested on SLSTR data on a range of environments.

2.2 The dual view on SLSTR

Due to the different path length, the dual view on SLSTR can be used for atmospheric correction as it is done in SLSTR SST algorithms using dual view (Merchant, 2012). Also Stroeve et al. (1996) demonstrated that the dual view improved IST performance compared to a split window algorithm. However, the swath width of the ‘nadir’ and ‘rear’ swath are not the same. The swath width ‘rear’ swath is about 740 km and the ‘nadir’ swath is about 1400 km and footprint sizes are not the same in the ‘nadir’ and ‘rear’ swaths. The ‘nadir’ swath is measuring at incidence angles between 0 (nadir) and 55 degrees. This will complicate efforts to take advantage of the dual view on the SLSTR instrument.

The dual view algorithm will combine different size and shape footprints and this mismatch can be quantified as part of the uncertainty. However, this component of the total uncertainty will not be estimated within this work. We will test both single view and dual view algorithms and if dual view algorithms are superior to single view algorithms, we will recommend to include both dual and nadir view IST products in the final output. The latter is to satisfy applications where frequent coverage is essential.

The dual view constellation still approximately satisfies the requirement of complete daily coverage (see Chapter 4) pole ward of 50 South and North, with one SLSTR instrument, provided clear sky. However, it is requested that product performance have higher priority that geographical coverage.

Figure 4 SLSTR dual view geometry (SLSTR Users Guide)

2.3 TIR emission from snow and ice

Clear-sky thermal infrared emission measured by satellite radiometers of snow-covered sea ice in the atmospheric window around 8 - 14 microns is primarily a function of the snow surface temperature and a number of other smaller factors affecting the measurement, including the snow surface emissivity. The snow emissivity at this wave-band is very close to 1, yet for large incidence angles (about 75 degrees) the emissivity decreases at wavelengths from about 11-13 microns by up to 1% due to variations in the ice permittivity (Dozier and Warren, 1982; Warren and Brandt, 2008). For wavelengths of about 10 to 12 microns, the emissivity variation is primarily due to viewing angle, and only secondarily to the surface snow grain size (due to scattering) and snow surface density (due to the scattering being affected by neighbouring scatters). The snow surface density is a measure of the packing density of snow grains, and neighbouring grains in the near field affect the scattering from other grains and the overall scattering magnitude, and thus to some extent the emissivity (Dozier and Warren, 1982). Snow grain sizes and snow density are not part of IST retrieval, but these factors can be used to quantify the relatively small and random noise caused by these two physical parameters in the IST retrieval algorithm and include it in the uncertainty estimate. The coefficients in the empirical temperature retrieval algorithms are tuned to the simulated emissivity resulting from average snow conditions and the magnitude of the emissivity.

It is difficult to measure the infrared emissivity of snow in the field, both because it is difficult to measure the actual snow surface temperature and because it is difficult to shield the measurement against reflected contributions from the sky and from the surroundings without changing the temperature of the measurement site at the same time. Attempts have anyway been made e.g. by Rees and James (1992) who

measured snow emissivity between 0.70 and 0.92. This large variation was measured even for snow of similar types. The low emissivity values in this emissivity measuring campaign compared to other measurements and large variability is probably due to the difficulty in measuring the physical temperature of the surface accurately. Hori et al. (2006) found that the snow emissivity is a function of both viewing angle and of snow grain size, and they further noticed that disaggregated snow had different emissivity than aggregated snow grains (sun crust). Hori et al. (2006) find the snow emissivity at nadir in the atmospheric window near 8-14 microns to be greater than 0.97.

2.3.1 Emissivity modelling

Emissivity modelling will be used for two things in this study: 1) for deriving one component in the uncertainty budget, and 2) as input to the atmospheric radiative transfer model RTTOV when calibrating the algorithm coefficients in the ice surface temperature algorithm.

Several models have been proposed and applied for the retrieval of snow grain sizes in the visual and near-infrared part of the spectrum, where sensitivity to grain size is larger than in the thermal infrared (Wiebe, 2011). At these relatively short wavelengths (compared to thermal infrared) near-field effects on the scattering are negligible, and the surface density (as a measure of grain packing density) and emissivity are independent (Dozier and Warren, 1982). In the thermal infrared, where the electromagnetic wavelengths are only an order of magnitude smaller or comparable to the snow grain size, the near field effects must be considered. We have implemented the Wiscombe and Warren (1980) model applied for simulations in the thermal infrared by Dozier and Warren (1982). Our implementation uses the updated pure ice refractive index table by Warren and Brandt (2008) covering the range of wavelengths from ultraviolet to the microwave derived for ice at 266 K. However, around 8-14 microns the temperature dependence on the permittivity is negligible. Linear interpolation is used in between individual table values in the Warren and Brandt (2008) table. The model uses Mie-scattering from uniform size ice spheres at the surface representing the effective optical snow grain size. Spectral response functions for each of the SLSTR channels are used for integration of the simulated spectral emissivity in the model.

One of the model assumptions is that the snow grains are a collection of equally sized spheres. Of course, in reality the snow grains on the surface are neither spherical nor do they all have uniform size. Precipitating snow crystal shapes are controlled by water vapour saturation and temperature and common shapes are hexagonal plates, columns and needles. However, when reaching the surface they may undergo mechanical break-up, if it is windy, which will tend to make them more spherical, and thermal gradient metamorphosis within the snowpack will make them grow in size (Marbouty, 1980). However, in the infrared the snowpack interior is not part of the emitting layer. An excellent discussion of the relationships between the dimensions of snow crystals measured in the field and the effective optical grain size is found in Aoki et al. (2007).

Input to our implementation of the model is viewing angle, electromagnetic wavelength, snow grain size, snow surface density, and physical temperature. In return, it simulates the directional and hemispherical emissivity, the radiance, and the brightness temperature using the Planck function. It uses the spectral response functions of the radiometer to integrate the spectral emissivity.

Using the emission model described in Dozier and Warren (1982) and the spectral response function for SLSTR A channel S8 (around 11 microns) we find that the differences in emissivity due to variations in snow

grain sizes between 50 and 200 microns is less than 0.00025 at nadir and less than 0.0006 at 55 degrees (figure 5). These numbers are relatively small compared to other error sources.

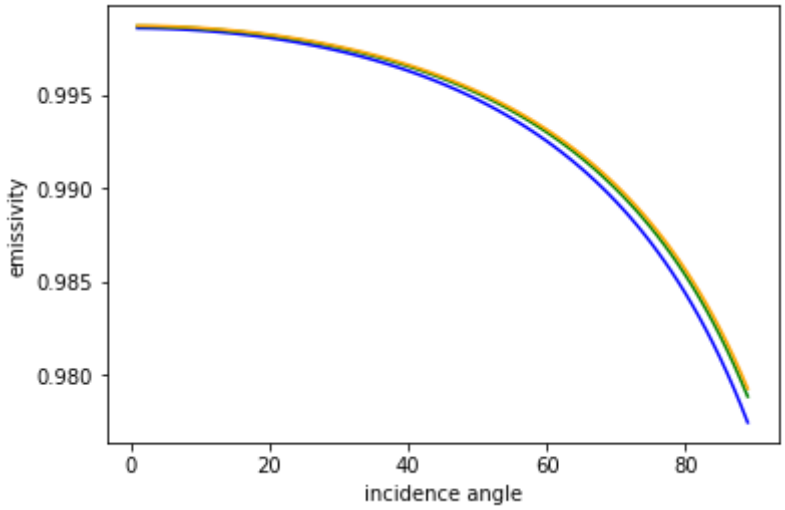

Figure 5: The S8 (11 microns) SLSTR directional emissivity as a function of incidence angle. The blue curve is for snow grain sizes 50 microns, green for 100 microns, and orange is for 200 microns. SLSTR is measuring at incidence angles between nadir and 55 degrees.

In addition, the 11(S8) and 12(S9) microns channel difference used in split window algorithms is most likely not due to different snow grain sizes as seen in figure 6.

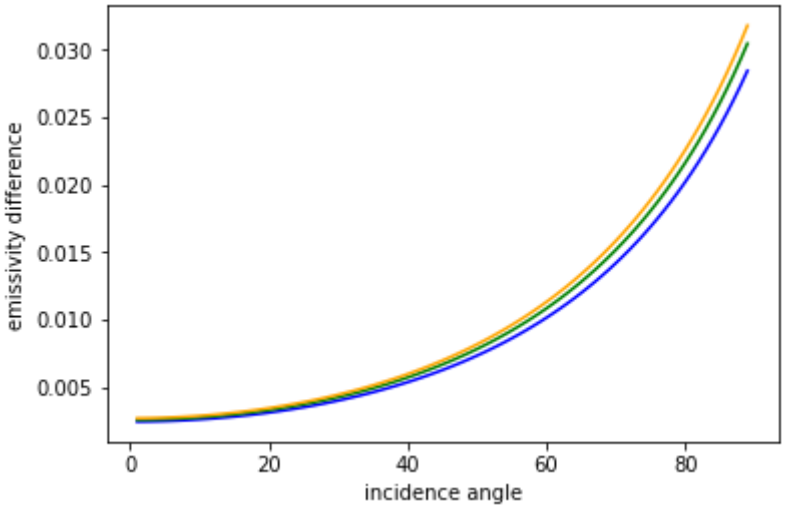

Figure 6: The 11(S8) and 12(S9) microns difference in directional emissivity for different snow grain sizes and incidence angles. The blue curve is the S8 and S9 emissivity difference for 50 microns snow grains, the green curve for 100 microns snow grains, and blue curve is for 200 microns snow grains.

2.4 Algorithm selection

A number of algorithms are described in Chapter 3 and some of these will be implemented and tested using the validation dataset. However, before selecting our candidate algorithm for SLSTR IST, we recommend the following studies:

Investigate the differences in the "nadir" and "rear" view Tb's, and how these are related to derived uncertainties, footprint mismatch, incidence angles, atmospheric path-length or other effects. In particular, it should be investigated if the dual view capability of SLSTR can be used directly for atmospheric correction.

Further, we will investigate to which extent the 11 (S8) and 12 (S9) microns Tb difference is related to atmospheric water vapour and snow grain size (snow grain size will be investigated using an emission model). According to Vincent et al. (2008b), the Tb difference at 11 and 12 microns is not related to atmospheric water vapour in the dry Arctic atmosphere.

Finally, we wish to test the feasibility of using methods for machine-learning regression for IST retrievals. While the below-described algorithms are based on physical principles, we will also look into the options of using IST algorithm in a more data-driven approach based on machine-learning regression principles. To our knowledge, this will be the first attempt to use such these methods for IST retrieval. Similar to the physically-based algorithms, calibration of the machine-learning regressions will be formed based on simulated observations from radiative transfer modelling of the radiation exchange between surface and the top of the atmosphere (see next section), possibly combined with parts of the in-situ observations in the match-up database . We expect to focus primarily on two machine-learning approaches, namely random forest and neural networks, both well-known for their high applicability to a range of situations. However, due to the novel nature of such approach, we expect this to be primarily a feasibility study.

2.5 Algorithm Calibration

Calibration of the recommended algorithms will be based on radiative transfer modelling (RTM) of the exchange of radiation between the surface and the top of the atmosphere. Despite the fact that snow and ice surfaces are much more homogenous that land surfaces, the spatial and temporal variations of surface properties have significant impact on IST retrievals. Sea ice emissivity depends on temperature, view angle, snow density and atmospheric water content (ranging from a very dry atmosphere over closed ice areas to humid in sea ice areas with low concentration, like the Marginal Ice Zone), thus challenging the feasibility of using a single algorithm for all conditions. The model calibration using RTM will determine robust algorithm regression coefficients for typical regions with different surface emissivity properties and different atmospheric compositions of pressure and water vapour. The STD of regression residuals will represent the algorithm uncertainty for a given algorithm domain. The recommended IST algorithms to test are defined at the end of the IST algorithm review in section 3.5, below.

2.6 Recommendations

Based on the discussions in this section we recommend the following approach for the algorithm selection:

- To investigate if the "nadir" and "rear" view of SLSTR can be used directly for atmospheric correction and for uncertainties

- Using a model to investigate how the 11 (S8) and 12 (S9) microns Tb difference and the individual Tb's are related to atmospheric water vapour and snow grain size
- Use forward simulations to quantify and study components in the uncertainty budget
- The uncertainty budget will be derived using the same approach as implemented in the OSISAF IST production (Dybkjaer et al. 2018), where the total uncertainty is a function of synoptic-scale, large-scale and random uncertainties

3 Review of IST products and processors

In the past four decades, satellite-based algorithms for land, sea and ice surface temperature retrieval algorithms have more or less been developed in parallel, using conceptually identical formalism, namely physically-based algorithms that are calibrated with empirical coefficients. The majority of the previous studies have addressed sea surface temperatures algorithm development and the least focus has been on ice surface temperature retrieval. Optimal Estimation (OE) algorithms are fundamentally different and are used for IR SST and PMW SST. EO algorithms are not considered here, but they could be subject for later studies.

Ice Surface Temperature is not an established surface temperature (ST) variable like Sea Surface Temperature (SST) and Land Surface Temperature (LST) that both are recognized as Essential Climate Variables (ECV) by the Global Climate Observing System (GCOS, 2019). The reason for this is probably that high uncertainties are associated with satellite IST products. This uncertainty is primarily caused by difficulties in detection of clouds over ice surfaces.

Some LST communities consider IST as part of their domain, because sea ice and ice sheet surfaces have similar radiative properties, and ice and snow is therefore treated as a separate land-cover type that also applies to sea ice areas. Today several dedicated satellite IST products are produced and available as monthly, weekly and daily products and some as level 2 swath products. The algorithms applied for generating IST are based on similar physical considerations as in TIR-based SST and LST algorithms (see section 3.2), which is the reason for including some references to LST and SST literature in this document.

Three types of IST algorithms exist, 1) TIR based algorithms, 2) MicroWave (MW) based algorithms, and 3) Mixed TIR and MW algorithms. The following is not a complete review of these IST algorithms – however all existing IST algorithm concepts are outlined and a review of TIR IST retrieval history is given attempted.

This chapter will, based on the IST algorithm review below and the discussions in Chapter 2, recommend a series of IST algorithm to be tested using the SLSTR instrument. Non TIR algorithms are also mentioned, and it is argued why it is not recommended to mix MW data in TIR based IST algorithms, despite the atmospherically transparent nature of MW radiation.

3.1 Major issues

There are three major challenges in TIR based surface temperature monitoring from space, namely: 1) screening of clouds, 2) atmospheric attenuation of the surface radiation, and 3) determination of surface emissivity, ε_s.

Cloud screening can be done successfully where the Earth's surface is warm relative to cloud top temperature and where visible (VIS) and Near/Mid IR (NIR/MIR) data are available for the cloud screening procedures (Hutchison et al., 2013). During polar night in Polar Regions, where only thermal infrared data is available for cloud screening, there are large uncertainties related to cloud detection, due to the similarity between surface and cloud top temperatures (see figure 3). The screening of clouds shall not be solved by the surface temperature algorithms, because clear sky is a prerequisite of using TIR algorithms for surface measurements, but the applied cloud screening technique determines to a large extent the quality of the IST product.

Atmospheric attenuation of the surface radiance distorts the signal received by the satellite at the Top-Of-the-Atmosphere (TOA). Even in the infrared window channels, atmospheric water will absorb and re-emit part of the surface radiation, resulting in a (mostly) colder temperature signal than originally emitted from the surface. This is also called the atmospheric temperature deficit (Zhang et al., 2009b). The atmospheric temperature deficit occurs because the absorbed and re-emitted surface signal now reflects the atmospheric temperature from where it is re-emitted. The surface temperature algorithm must deal with variations in atmospheric water content because of potentially large spatial and temporal variability of atmospheric water. Water vapour correction terms are discussed in the review of the TIR algorithms.

The determination of **surface emissivity** is another variable that is hard to determine accurately and that influences the quality of surface temperature estimate, even for snow and ice that appear rather homogeneous. The emissivity does, as mentioned in section 2.3, depend on snow grain size, snow density and on the wavelength of the surface emittance (Dozier and Warren 1982), but also on the view angle. Surface emissivity must be dealt with by the surface temperature algorithm, despite the fact that it is not realistic to obtain information of the spatial and temporal variation of e.g. snow grain size and snow density.

The following section describes the development of infrared surface temperature algorithms in general, and mentions the most acknowledged IST algorithms and how they deal with the issues mentioned above. Alternative IST algorithms are mentioned and it is argued why such algorithms are not suited for precise IST monitoring. Finally, a list of recommended SLSTR IST algorithms is given.

3.2 TIR IST algorithms

The first surface temperature maps from satellite data were made after launch of the early meteorological Nimbus satellite in the 1960's, with the High Resolution (mid) Infrared Radiometer (HRIR). This was a simple grey-tone temperature map scaled to typical ocean temperatures (USSSP, 1972). Soon after the early grey-tone map technique, satellite monitoring of earth surface temperatures was developed into the simplest form of the physically-based regression model that conceptually still applies: A linear scaling between IR brightness temperature (*Tb*), and surface temperature, T_s. This was made possible with the launch of the thermal infrared Scanning Radiometer (SR) on board TIROS-M and NOAA-1 satellites (LaVioletta and Chabot, 1968; Rao and Strong, 1971).

Equation 1

$$T_s = a_0 + \sum_{i=1}^{n} a_i Tb_i$$

Equation 1 is the general expression for many TIR-based surface temperature algorithms, applied since the first SR-based algorithm. Here, T_s is the surface temperature, n is the number of *Tb* channels applied and Tb_i refers to the i^{th} channel, and a_i is the corresponding calibration coefficients.

In the simplest case (n=1), as for the SR instrument, a_1 is proportional to $1/\varepsilon_s$ and a_0 is a constant temperature correction that, among other things, corrects for an average atmospheric temperature deficit. This algorithm will of course introduce large uncertainties given temporally and spatially variations in atmospheric water content and surface emissivity.

Later it was shown that if using n>1, equation 1 will dynamically adjust for atmospheric water under the assumption that the atmospheric attenuation is small and that errors caused from this can be considered linear. Here it is also assumed that the snow emissivity for the applied Tb_i wavelength are identical and they are spectrally close, so that the Planck function can be considered linear (Zhang et al., 2009a, Zhang et al., 2009b). The argument is that the difference between 2 *Tb'*s is mainly a function of atmospheric water content. The relationships between the corresponding a_i coefficients are hence a relative measure of the atmospheric water absorption (Price, 1984; Stroeve et al., 1996).

It has been shown that equation 1 also applies for *Tb*'s at identical frequencies, but at different view angles for dry atmospheres, which usually is the case in Polar Regions (Zavody et al., 1995; Stroeve et al., 1996; McMillin, 1975). This makes equation 1 generally applicable for common multispectral satellite sensors and for SLSTR and earlier dual view sensors as well (i.e. ATSR and AATSR).

Under the assumptions mentioned above, the a_i coefficients in equation 1 are physically derivable variables of surface emissivity, view angle and atmospheric reflectivity or transmittance (Remedios and Emsley, 2012; Zavody et al., 1995), but the coefficients are usually determined statistically from regression analysis. The data applied for regression analysis are either measured surface temperatures and corresponding satellite measurements, or modelled surface temperatures and corresponding modelled TOA radiances that are determined from applying NWP data in a radiative transfer model (RTM). The latter method for tuning of coefficients is the most commonly used. This is to circumvent issues with erroneous and sparse in situ measurements from Polar Regions, and atmospheric contaminated satellite data, e.g. from non-detected cloud cover.

Most surface temperature algorithms operating today are slight modifications of equation 1, modified in order to account for non-linearity in the relation between ST and TOA radiation. This is usually done by adding terms including satellite view angle to adjust for view angle dependent emissivity of snow and ice (Dozier and Warren 1982; Hori et al., 2013). This and other variations of equation 1 are described below in section 3.2.1, where a review of existing IST algorithms is given.

3.2.1 Applied TIR-based algorithms

This section reviews TIR-based snow and ice surface temperature algorithms that have been reported in the scientific literature. Not all IST algorithms are included, but all conceptually unique and high performance algorithms are mentioned, as well as essential operational state-of-the-art operational products are listed.

Until the beginning of the 1990's no dedicated IST algorithm were operating, to our knowledge. Snow and ice surfaces on land were only monitored by LST algorithms, but sea ice temperature monitoring was not reported.

By the launch of NOAA 7 in 1981, with the Advanced Very High Resolution Radiometer (AVHRR/2) on-board, the first dual TIR channel was put in operation. Since then, the amount of literature on surface temperature monitoring increased drastically for LST and SST algorithms. The first LST algorithms that used AVHRR/2 data were identical to equation 1, with n=2 (Price 1984; Wan and Dozier 1989). They showed improved surface temperature precision by exploiting the two TIR channels for atmospheric correction.

The first dedicated IST algorithm included a view angle correction to the equation 1 (n=2) algorithm. The algorithm is shown in equation 2, and was published by Key and Haefliger (1992). They included the non-linear view angle term to avoid a piecewise tuning of equation 1, in ranges of view angles that would be an alternative means to correct for view angle dependent emissivity.

Equation 2

$$T_s = a_0 + a_1 Tb_{11} + a_2 Tb_{12} + a_3\big((Tb_{11} - Tb_{12}) sec\ \theta\big)$$

Here, Tb_{11} and Tb_{12} are TIR brightness temperature channels centred at ~11 microns and ~12 microns, channel 4 and 5 of the AVHRR/2 instrument, respectively. Sec Θ is the secant of the satellite view angle. Key and Haefliger (1992) also considered temperature dependency of the algorithm by tuning the a_x coefficients seasonally, and thus dealing with non-linear temperature-dependent relations. Equation 2 was also tested for various combinations of view angle dependency (e.g. (Sec Θ - 1) instead of Sec Θ), but the relation in equation 2 was chosen for temperature estimation for Central Arctic sea ice.

This model was also applied by Lindsay and Rothrock (1993) and Haefliger et al. (1993), for Chuckchi Sea and Greenland Ice Sheet.

Key et al. (1997) later performed a minor change to equation 2 for AVHRR data and for ATSR data for comparison. They applied equation 2 with 2 spectrally different TIR channels from AVHRR and 2 spectrally equal TIR channels with different view angles from ATSR, as stated to be a feasible application for the general algorithm (equation 1). These algorithms are shown in equation 3 and 4. Equation 2 and 3 only differs by an alternative angular dependency term, where (Sec Θ -1) replaces Sec Θ.

Equation 3

$$T_s = a_0 + a_1 Tb_{11} + a_2 Tb_{12} + a_3\big((Tb_{11} - Tb_{12})(sec\ \theta - 1)\big)$$

Equation 4

$$T_s = a_0 + a_1 Tb_{11nadir} + a_2 Tb_{12nadir} + a_3 Tb_{11forward} + a_4 Tb_{12forward}$$

In equation 4, *nadir* and *forward* represent the ATSR nadir-looking and forward-looking sensors, respectively. The Key et al. (1997) algorithm was tuned piecewise within 3 temperature ranges of annual ice surface temperatures, to circumvent non-linear temperature dependencies. The approach in equation 3 apparently performed better than the earlier version (equation 2) for AVHRR data. The equation 3 and 4 algorithms, performed comparable using AVHRR and ATSR data. ATSR with larger (negative) bias than the AVHRR algorithm, but the AVHRR algorithm showed a slightly larger STD of differences, than the ATSR algorithm. RMSE between 4 and 5 K were reported.

The absence of major improvement using dual view is explained by the dry Arctic atmosphere, and a subsequent less significant advantage for the dual view sensor algorithm. Stroeve et al. (1996) made an inter-comparison between an ordinary split window algorithm (equation 1 for n=2 at 11 and 12 microns), the equation 4 algorithm (= equation 1 for n=4) and finally a single frequency algorithm with dual view (equation 1 for n=2 at 11 microns dual view, equation 5), using ATSR data. They found that both dual-view algorithms performed superior to the traditional split window algorithm for IST on the Greenland Ice Sheet.

Equation 5

$$T_s = a_0 + a_1 Tb_{11nadir} + a_2 Tb_{11nadir} + a_3 Tb_{11forward}$$

Stroeve and Steffen (1998) also applied equation 3 for a temperature analysis for the Greenland Ice Sheet for the period 1989 to 1993. They reported STD errors between 1 and 2 K, primarily caused by undetected clouds. Manual cloud screening in this study resulted in the relative low error range.

A study from Veilemann et al. (2001) tested a one channel algorithm (algorithm 1, n=1) for the Weddell Sea in the southern hemisphere. Here, clouds were screened manually and the coefficients were for individual data points using RTM to correct for the atmospheric influence. They reported standard errors around 2.5 K.

The Moderate-resolution Imaging Spectro-radiometer (MODIS) instruments on Terra (launched in 1999) and Aqua (launched in 2002) have the same TIR channels as the AVHRR/2 instrument, but at the same time it is a multi-spectrometer with better cloud detection potential than AVHRR. Soon after launch, NASA established dedicated IST products in level 2 and 3 by applying the Key et al. (1997) algorithm (Hall et al., 2001). The MODIS IST products have since been subject to a number of publications on Greenland ice sheet temperatures (Hall et al. 2004a, 2012, and 2013) and sea ice temperatures (Hall et al. 2004b).

In a comparison study between AVHRR and MODIS IST using the algorithm in equation 3, and compared against radiometric in situ observations, no significant performance differences were found (Scambos et al., 2006). Standard errors were around 1.4 K, using manually determined cloud-free conditions.

While the older AVHRR and MODIS instruments are still operating, NASA launched in 2011 the Visible Infrared Imaging Radiometer Suite (VIIRS) sensor, to become the natural continuation of the long lasting AVHRR time series and at the same time to provide operational continuity of the MODIS multi spectrometer. VIIRS is a superior instrument (spectrally and spatially) than both the AVHRR and MODIS instruments.

NOAA/NESDIS (2019) adapted the Key et al. (1997) algorithm for IST to the VIIRS bands M15 & M16 that are comparable to the 2 TIR channels on AVHRR at ~11 and ~12 microns (Key et al. 2013). The NOAA/NESDIS VIIRS IST performance against drifting buoys was estimated to be approximately 3.7 K.

In 2012, an IST product using Metop AVHRR data was implemented using the equation 3 algorithm (Dybkjaer et al. 2012). This product showed performances between 3 and 4 K when compared to Arctic drifting buoys and air temperatures from land-ice based Automatic Weather Stations (AWS). When compared to radiometric in situ observations in clear sky conditions, the standard errors were less than 1 K. This product was in 2016 further developed and enrolled in the Ocean and Sea Ice, Satellite Application Facility (OSISAF) product portfolio (Dybkjaer et al. 2018). The OSISAF algorithm is identical to equation 3.

As part of a field study concerning ESA's Fiducial Reference Measurements (FRM) of sea ice, a satellite IST product inter-comparison was made between Metop AVHRR (OSISAF, Dybkjaer et al. 2018), NPP SUOMI VIIRS (National Polar-Orbiting Environmental Satellite System (NPOESS), Liu et al. 2015) and Aqua and Terra MODIS (NASA-GSFC, Hall et al. 2004b). All four products are based on identical algorithms, namely the Key et al. (1997) algorithm.

Closest pixel	Metop_A AVHRR	VIIRS	MODIS TERRA	MODIS AQUA
Mean difference	- 0.4 K	-1.7 K	-1.4 K	-1.9 K
Median abs difference	0.8 K	1.5 K	0.8 K	1.1 K
RMSE	2.0 K	3.6 K	3.5 K	4.8 K
stdv (differences)	1.9 K	3.2 K	3.3 K	4.4 K
N(matches)	227	197	122	165

Table 1 Statistics from DMI AWS radiometric Ice surface temperatures from sea ice, and the closest pixel of Metop-A, AVHRR VIIRS MODIS Terra and Aqua for the period between January and June 2016 (from Høyer et al., 2017).

Results from the study are shown in table 1, where the retrieved IST of the closest pixel for each product is matched up with radiometric skin temperatures from the DMI AWS in a fast ice region located approximately 10 km from Qaanaaq in North West Greenland. All products use their associated automatic cloud masks, which most likely are the main cause of the different performance statistics of the products, which ranges from STD of differences of 1.9 K for Metop-AVHRR to 4.4 K for MODIS Aqua. To our knowledge, the four products (Metop AVHRR, VIIRS, MODIS Aqua and Terra) are the only existing operational level 2 IST products for sea ice.

An operational Sentinel-3 SLSTR LST algorithm including snow surface temperature has been formulated using a general LST algorithm for all land cover classes (Remedios and Emsley 2012). The SLSTR LST algorithm is conceptually close to the only operational TIR IST algorithm applied today (equation 3), but with a slightly different approach to handle view-angle-dependent non-linearity. They introduced a view angle dependent exponential term, including a land cover specific variable (equation 6).

Equation 6

$$T_s = a_0 + a_1(Tb_{11} - Tb_{12})^{1/(cos(\Theta/lc))} + a_3 Tb_{12}$$

Θ is the satellite view angle and *lc* is a land-cover type specific variable that determines the weights of the non-linearity term of the given land cover. This is very similar to equations 2 and 3, with the difference that the sensitivity can be locally configured, using the *lc* variable.

3.3 Non-TIR IST algorithms

A few satellite-based IST products are conceptually different from the TIR based products, e.g. surface temperature algorithms from Comiso et al. (2003) and Hwang and Barber (2008). These are based on microwave emission in the vertically-polarized 6.9 GHz channel of the AMSR instrument, using an estimate for the surface emissivity at this wavelength, and the sea ice concentration.

The ice temperature derived in this way represents the physical temperature of the layer that emits radiation at this wavelength. Under some circumstances, depending mainly on snow depth, density and moisture, the penetration depth can be deep, and the estimated ice surface temperature can be far from the snow skin temperature (Hwang and Barber, 2008). For first-year sea ice, the 6.9 GHz ice temperature is

shown to be a good proxy for the snow-ice interface temperature (Tonboe et al., 2011), since a dry snow cover is almost transparent to the radiation at this frequency, while the ice is opaque due to the high salinity of first-year sea ice. For multi-year ice, the temperature represents a weighted average of the free-board portion of the ice, which may also be reasonably close to the snow/ice interface temperature (Comiso, 2003). During periods of snow melt, the microwave signal changes characteristics, and the MW ice temperatures deviates largely from the skin temperature (Hwang and Barber, 2008), due to the large variability in the physical snow properties, and consequently in the radiative penetration depth.

3.4 IST Algorithms based on combined TIR and MW data

A different approach using TIR and MW data for IST estimation is the EUMETSAT Piece Wise Linear Regression (PWLR) retrieval of various variables, including ice surface temperature (Hultberg & August, 20XX). The PWLR IST algorithm is based on a multi-linear-regression scheme including co-located IASI, AMSU and MHS data, paired with ECMWF analysis fields. Using a hierarchical approach, the training data was categorized into different retrieval classes, and within each, the relationship between observations and variables was represented by a linear fit, thereby offering a fast regression scheme.

3.4.1 MW data in IST processor is not recommended

The temperature gradient from the atmosphere through the snow and sea ice to the upper ocean is very steep. Air temperature during winter are -40 to -30 degrees and the water 2 m below the air is at the freezing point (-1.8 degrees). Microwaves penetrate the surface and the thermal microwave emission is an integrated brightness temperature for the upper snow and ice. There is a good correlation between the snow ice interface temperature and the 6 GHz brightness temperature because of penetration through the snow and an almost constant emissivity at 6 GHz. At higher microwave frequencies (23 and 36 GHz) the snow grains acts as scatters and the sea ice emissivity is highly variable, from day to day and from ice type to ice type. Even when the emissivity is known, the integrated temperature, which can be derived, has only a noisy relationship with the snow ice interface or the snow surface temperature. Further, the 23 GHz channel is affected by atmospheric water vapour absorption. However, this is difficult to quantify because there is no 18 GHz channel for comparison. The temperature, which can be derived from microwaves, is not the same as the snow surface temperature and inclusion of MW data in a TIR IST algorithm is not recommended.

3.5 Recommendations

This review shows how existing TIR based snow and ice temperature algorithms are developed from conceptually identical assumptions and that the algorithms differ in their way to handle non-linear features.

For the SLSTR IST retrieval algorithm development, we recommend to test existing IST retrieval concepts that are based on TIR data only. In chapter 2 it is argued why we recommend excluding MW data as additional satellite input to IST retrieval, as attempted by others. Furthermore, it is described how earlier IST retrieval works argue for and against split window algorithms. Some suggest that an atmospheric correction term applied in the dry Polar Regions, using split window, is needless, and others describe improved performance of IST algorithms when including atmospheric correction. In the literature, several authors include an angular dependent emissivity correction term with success, which is confirmed to make good sense in the discussions of Chapter 2.

We recommend a systematic analysis of a series of algorithms, starting from most simple linear retrieval algorithm concept from equation 1 and gradually adding non-linear terms to multi sensor split windows window algorithms.

We recommend testing six algorithms in total. We recommend testing:

- A 1 channel algorithm with fixed view angle in order to circumvent non-linear angle dependencies (equation 1, for *n* = 1 being $Tb_{11oblique}$)
- A split window algorithm with fixed view angle to adjust for atmospheric water (equation 1, for *n* = 2 being $Tb_{11oblique}$ and $Tb_{12oblique}$)
- A split window algorithm with view angle correction terms (equation 3) that is calibrated within 3 temperature intervals to circumvent non-linear temperature dependencies (calibration in cold temperatures: $Tb_{11nadir}$<240K; in medium temperatures: 240K< $Tb_{11nadir}$<260K; and in warm temperatures: $Tb_{11nadir}$>260K):)
- A combined dual view and split window algorithm (equation 4)
- A LST algorithm (equation 6), for comparison. Calibration will be performed with fixed LandCover (lc) weight parameter from University of Leicester (Darren Ghent) and with 'lc' as regression parameter:
- A new algorithm (equation 7, see below), which is equation 4 with the addition of a view angle dependent emissivity correction term.

Equation 7

$$T_s = a_0 + a_1 Tb_{11nadir} + a_2 Tb_{12nadir} + a_3 Tb_{11oblique} + a_4 Tb_{12oblique} + a_5\left((Tb_{11} - Tb_{12})(sec\ \theta - 1)\right)$$

The equation 7 algorithm now includes the full complexity from current and previous IST algorithms in 1 algorithm, which is equation 1 for n=4, plus an angular correction term. Six algorithms will be tested.

It is essential to map the performance enhancement for each step of algorithm complexity and evaluate to what extent split window and dual view and angular dependency can add to improving total performance.

3.5.1 Test algorithm summary

Hence, following Six SLSTR IST algorithms are recommended for testing, SLSTR-IST1 to SLSTR-IST6:

SLSTR-IST1:

$$T_s = a_0 + a_1 Tb_{11\mathrm{oblique}}$$

SLSTR-IST2:

$$T_s = a_0 + a_1 Tb_{11oblique} + a_2 Tb_{12oblique}$$

SLSTR-IST3:

$$T_s = a_0 + a_1 Tb_{11\mathrm{nadir}} + a_2 Tb_{12\mathrm{nadir}} + a_3\left((Tb_{11\mathrm{nadir}} - Tb_{12\mathrm{nadir}})(sec\ \theta - 1)\right)$$

SLSTR-IST4:

$$T_s = a_0 + a_1 Tb_{11nadir} + a_2 Tb_{12nadir} + a_3 Tb_{11oblique} + a_4 Tb_{12oblique}$$

SLSTR-IST5:

$$T_s = a_0 + a_1(Tb_{11\text{nadir}} - Tb_{12\text{nadir}})^{1/(cos(\theta/lc))} + a_2 Tb_{12\text{nadir}}$$

SLSTR-IST6:

$$T_s = a_0 + a_1 Tb_{11nadir} + a_2 Tb_{12nadir} + a_3 Tb_{11oblique} + a_4 Tb_{12oblique} + a_5\big((Tb_{11\text{nadir}} - Tb_{12\text{nadir}})(sec\ \theta - 1)\big)$$

The number algorithms that will end up in the ATBD version 1 (working document) and subsequently will be tested in the Validation Report, may very well differ from these 6 recommended algorithms, but they will be in algorithm "family" with the 6 recommended. For example, we might end up testing equation SLSTR-IST1, using both nadir and oblique view.

4 General requirements

The production of geophysical variables is usually subject to a number of requirements from users, scientific societies, producers and other stakeholders relevant to the product. This naturally goes for the SLSTR IST product and production as well.

We have identified a number of general requirements from acknowledged organisations and stakeholders related to the SLSTR IST product. It is not a complete list of IST related requirements, but a list of essential requirements that are relevant to the IST processor, product, performance and output.

In section 4.1 is a list of all relevant requirements from following organizations and societies: Copernicus/CMEMS, GHRSST (2012), National Research Council (NCR, Abbott 2000), Climate and Cryosphere (CLiC 2012), Generic Specification of Work (GSoW 2018), GMES Sentinel-3 mission (Donlon et al. 2012), GMES MCS Implementation Plan, Global Climate Observing System (GCOS), Requirements for ocean observations (Stammer, 2007), Radiometric Temperature Measurements (RTM, Zhang 2009b), and Sentinel-3 Mission Requirements Traceability Document (MRTD and MRD).

Each requirement in the list is commented on how it will be met. In Section 4.2 special attention has been given to IST performance requirements. Here it is discussed where the requirements originates from and whether it can be met. It is also discussed how other products handle IST performance requirements.

Input/Output (IO) requirement issues are found in Chapter 5, where all IO data are listed and output format requirements are discussed.

In Chapter 6, all identified requirements are summarized in a table.

4.1 Requirements by stakeholder

Requirements from all identified SLSTR IST stakeholder organizations and other relevant parties.

Copernicus/CMEMS

- SLSTR data from Sentinel-3 A, B and C applied for Sea Ice monitoring in near real time (CMEMS, 2020)
    - The NRT requirements is met in the level-2 prototype processor
- Output must comply with the L2P specifications (CMEMS, 2020)
    - Requirement will be met (see section 5.4)
- Better monitoring of rapidly changing Polar Regions is needed (CMEMS, 2017).
    - Polar monitoring is enhanced with this project
- Monitoring at diurnal scale is required at 1 km resolution and at 10 % accuracy (a percentage indication of accuracy does not make sense in this context)
    - The level 2 IST output is based on original swath resolution of 1 km at nadir.
- Dedicated in situ activities are needed to ensure the acquisition of the Fiducial Reference Measurements (FRM) needed for the calibration and validation of satellite sensors and derived products (CMEMS, 2017).

    - This is in line with statements in section 5.2 regarding uncertainties from different in situ sources. We recommend to exclude traditional drifters (e.g. from drifter data from ECMWF in situ archive), due to their un-traceability and high uncertainty. We recommend to focus cal/val on land based weather stations (e.g. ARM and PROMICE), and high quality drifter data from e.g. Ice Massbalance Buoys or manned field campaigns.
- Copernicus Polar mission user requirement emphasize the importance of sea ice and land ice surface temperature monitoring (Copernicus, 2018a).Here, Ice-surface temperature is stated potentially as important as the SST in terms of assimilation for vertical heat diffusion
- Specific IST requirements for sea ice ST and ice cap ST are: temperature range 173-290, timeliness of 1 hour, accuracy 0.5 - 1 K, frequency 6 hourly and a spatial resolution of 5 – 10 km (Copernicus, 2018a)
    - The temperature range prepared for the SLSTR IST prototype processor is 165-300 K and thus full compliancy.
    - Timeliness is approximately 15 minutes plus SLSTR data availability at the processing center.
    - Frequency is approximately bi-hourly in the Polar Regions, for cloud free areas.
    - Spatial resolution is 1 km at Nadir
- Requirement for Pan-Arctic IST monitoring at sub daily frequency for diurnal cycle monitoring (Copernicus, 2018b). The spatial sampling is required to be maximum 5 km.
    - This is achieved through level 2 processing, which means multiple daily coverage in Polar Regions at approximately 1 km resolution at nadir.
- In a gap analysis in a CMEMS position paper (CMEMS, 2016) and a Copernicus user requirement document (Copernicus, 2018b) it was identified that no SLSTR IST product for sea ice is foreseen
    - This is reimbursed with this project.

GHRSST

- The output file format shall follow the well documented GHRSST format, GDS2.0, including distributed Single Sensor Error Statistics (SSES) of both bias and standard deviation (STD)
    - Requirement will be met (see section 5.4)
- Product Output data format in NetCDF4
    - Requirement will be met (see section 5.4)

National Research Council

- Traceability for validation
    - Requirement will be met where possible (see Radiometric Temperature Measurements)
- Quality assessment shall be an intrinsic part of operational data production
    - The product will be validated (see PVP), an uncertainty algorithm will be developed (see below) and quality levels will be assigned following GHRSST standards
- For purposes of data continuity the SLSTR IST product should overlap with at least 1 year of other products
    - One year OSISAF IST will be added to the validation procedure (See PVP)
- The system should have the ability to re-process large data sets

    - The production will based on generic and documented program Code that can be read and adapted to fast reprocessing by skilled programmers, if necessary

Climate and Cryosphere

- NetCDF or other standard output format
    - Requirement will be met (see above)
- Uncertainty – preferable space and time dependent
    - The uncertainty budget will be closed using the same approach as implemented in the OSISAF IST production (Dybkjaer et al. 2018), where the total uncertainty is a function of synoptic-scale, large-scale and random uncertainties

Generic Specification of Work

- An IST performance requirement of 1 K
    - This is not likely to be fulfilled, however it is expected that uncertainty components induced by random noise (NEdT), geolocation error and algorithm regression residual will improve relative to the OSISAF IST product. See also section 4.2
- Seamless interface across the MIZ
    - This is planned to be solved with similar approach as in the OSISAT IST production, by applying interpolation between IST and SST in the MIZ (Dybkjaer et al. 2018)
- Consider outcome of cloud screening over sea ice
    - This is met by implementing an additional cloud screening procedure from Leicester's SLSTR LST production
- Uncertainty model
    - Requirement will be met (See CLiC)
- Min. 6 month data
    - One year of validation data is planned (See PVP)
- Comply with GHRSST data format
    - Will follow the GHRSST data format and OSISAF IST output standards
- Comply with OSISAF OSI-205 IST output standards
    - yes

GMES Sentinel-3 mission

- Focus on inter-calibration between successive sensors and long-term validation for climate consistency
    - Sentinel-3 A and B will be inter-compared for a half year period and further compared with OSISAF IST product is planned in the PVP

GMES Marine Service and operational oceanography service requirements taken from the GMES MCS Implementation Plan:

- Performance: Ice Surface Temperature 1 K (10 %) < 5 km (1 km goal)
    - See section 4.2
- Timeliness: NRT

    - This should not be a problem
- Frequency: Daily
    - This will be met, because SLSTR provide multiple daily coverage pole wards of 50 degree North and South

GCOS

- A suitable period of overlap with existing systems
    - Will be done (See above (GMES and SoW))
- High priority for additional observations should be in focus in data-poor regions
    - This is planned. See PVP
- Earth systems should be sampled in a way that climate relevant changes can be resolved – i.e. diurnal, seasonal, inter-annual and long-term changes
    - This is fully applicable with the level 2 product that is planned
- Uncertainty budget
    - Requirement will be made (See CLiC)

Requirements for ocean observations

- An IST performance requirement of 1 K
    - This is not likely to be fulfilled, however it is expected that uncertainty components induced by random noise (NEdT), geo-location error and algorithm regression residual will improve relative to the OSISAF IST product. See also section 4.2

Radiometric Temperature Measurements (Zhang 2009b)

- RTM tuning of algorithm in data poor regions
    - This is planned
- Traceability of in situ observations
    - Full traceability of most common in situ temperature is not possible, but the inclusion of land stations like the PROMICE and ARMS station does to some extent comply with this requirement

MRTD and MRD

- 'Land Colour and Temperature' for land surface (including sea ice and ice sheets), with complete Earth coverage in 1 to 2 days, with products at least equivalent to those derived from ENVISAT MERIS, AATSR
    - Planned
- Performance: Space time coverage requirements for the Sentinel-3 SLST instrument shall take second priority with respect to absolute accuracy requirements
    - ok
- Performance: Sentinel-3 shall be able to measure Ice Surface Temperature (IST) to an accuracy of 10 % with a resolution of < 5 km (1 km goal) at nadir. This capability shall not reduce the quality of the SST retrievals

    - It is not clear what and accuracy of 10% means, but we assume it is 10% of a given temperature range. See section 4.2
- Geographic Coverage: Sentinel-3 Ice Surface Temperature (IST) products shall have complete global coverage over ice covered surfaces including oceanic, coastal waters and inland seas.
    - Planned
- Spatial resolution: Sentinel-3 SST, IST and LST measurements shall have a spatial resolution of = 1000 m at nadir
    - Spatial resolution will be FOV, i.e. 1 km at Nadir
- Timeliness: Sentinel-3 products for GMES Services shall be made available according to the timeliness requirements described in Table 17 and Table 18
    - Planned
- Service Data Products: Sentinel-3 shall provide data products in acceptable formats used by operational NOP and NWP systems (e.g., netCDF, L2P, BUFR)
    - Planned. See Section 5.4
- Performance: Ice surface Temperature 1 K (10 %) < 5 km (1 km goal) Daily (TABLE 14)
    - See section 4.2

4.2 IST performance requirements

There seem to be a consensus around the performance requirements for satellite based IST products, of 1 K, not always further specified. In the section below it is attempted to trace this requirement to its origin. It turns out that the original 1 K requirement was aiming at a mean area temperature precision and that it is necessary to stratify requirements into both observations type other validation “regimes”.

In section 4.2.2 it is explained how requirements are split into observation type and in section 4.2.3 it is explained how the performance analysis is recommended carried out for the SLSTR IST.

4.2.1 Consensus requirement for IST

Various documents concerning the requirement of IST performance and spatio-temporal coverage seem to agree on performance requirement, namely that STD of IST uncertainty must be less than 1 K. This is reflected in the MRTD document, in Stammer et al. (2007) and in the WMO rolling requirement archive that is part of the Observing Systems Capability Analysis and Review Tool (OSCAR) project. However, these sources all trace back to an Arctic Climate System Study (ACSYS) project document under the World Climate Research Programme (WCRP).

According to WMO the original requirements were stated by the CLImate and Cryosphere project (CLIC), writing that the IST performance requirements should be 1.0 K, 1.3 K and 2.0 K, at Goal, Breakthrough and Threshold requirements, for 100 km, 200 km and 500 km averages, respectively, and the corresponding data coverage should be 12 h, 18 h and 24 h. The term Goal is the ultimate precision and Threshold is the worst performance for which information still can be applied. Breakthrough is an intermediate performance requirement. Both Goal and Breakthrough requirements may be within reach for the SLSTR IST under certain conditions, however representative average IST values for 100 km, 200 km and 500 km grids are not easily determined. The original ACSYS requirement text (a possible 1998 reference) was unfortunately not possible to acquire.

The original ACSYS requirements have subsequently been subject to interpretations, e.g. to a daily STD of differences of 1 K, at 1 km requirement in the MRTD document, and a Root Mean Square Error requirement of 2K/1K/0.5K at 500km/100km/25km (Break/Breakthrough/Threshold) for climate monitoring in Stammer et al. (2007). Also in Stammer et al. (2007) a user analysis was carried out for global NWP model applications, here Break/Breakthrough/Threshold were set to 4K/1K/0.5K at 250km/25km/5km grids.

4.2.2 OSI-205 IST

The requirements for the OSISAF IST product (OSI205) are summarized in the PRD document (PRD-OSISAF). Here the performance of the IST is split into validation against traditional buoys measurements and radiometric skin temperature measurements, where the Target requirements are 3 K and 2 K, respectively, and the corresponding maximum mean error requirements are 3.5 K and 1.5 K. The level 2 product timeliness requirement is 3 hours from acquisition and spatial resolution is the sensor Field of View. It is explained in Chapter 1 how the buoy in situ measurements are much less trustworthy that radiometric surface measurements, but they are included in the validation procedures to enhance in situ data the volume.

With respect to the STD and mean requirements, it must be required that the SLSTR IST performs better than OSI205. However, in addition to stratification of validation into radiometric and buoy observations, validation of the SLSTR IST must be further stratified into total performance and total performance in positively clear sky situations. The latter is important, because the cloud screening products used on SLSTR data over ice are conceptually different from traditional cloud mask applied with the OSI205 product and other existing IST products. Validation in “positively clear sky situations” can be carried out for AWS observation data with radiation balance measurements, for which a qualified cloud fraction estimate can be calculated.

Based on experience from the OSI-205 product, we recommend that the Threshold, Target and Optimal accuracy requirements be carried on the SLSTR IST performance requirements. The reason for this is that there is no reason to believe that the SLSTR cloud screening presently is superior to the cloud screening performed for the OSI-205 product, in Polar Regions.

4.2.3 Stratified performance requirements

The estimated sampling and instrument uncertainty statistics from table 2 can be exploited to actually compare validation statistics from buoy measurements with statistics from radiometric surface temperature measurements. The in situ instrument uncertainty will be subtracted from the product performance statistics for the respective type of in situ observation. This is similar to the validation process for the Metop IST product in the OSISAF, where validation requirements are stratified between temperature observations from buoys and from radiometer.

Beside, stratification of performance into observation type we also recommend to stratify into positively clear sky conditions and “normal” performance. Within the monitoring and validation methodologies, it is possible to quantify the IST uncertainties in likely clear sky conditions. The total IST uncertainty will be described in the uncertainty algorithm, in which the uncertainty contribution from undetected clouds is an independent term that can be omitted.

The performance of the total IST uncertainty algorithm in positively clear sky conditions can to some extent be validated from land observations that estimate cloud fraction from radiation balance data. Such data are available from PROMICE stations (Greenland), ARMS stations (Alaska) and the DMI-AWS data from Qaanaaq (Greenland). Dedicated IST validations will thus be done for data screened with AWS cloud fractions (see performance of AWS cloud screening in figure 3).

We assume that a 1 K performance requirement will be challenging to reach for normal performance analysis, but the “clear sky” performance will be close to the 1 K requirement, when we compensate for observation uncertainty, as mentioned above.

A final requirement for SLSTR IST is to perform similar or better than current state-of-the-art IST products, e.g. the OSI-205 product.

5 IO data and requirements

Specific OI requirements from Chapter 4 are described here. The IO data requirements are divided into 3 different processes, 1) Input requirements for the SLSTR IST processor; 2) Requirements for in-situ data, and 3) Input requirements to the Match-Up DataBase (MUDB).

5.1 Input to MUDB

With respect to MUDB input data, then focus is on complying with the general requirements of quality, representativeness and traceability to the highest possible level. The following list is the planned content of the MUDB. This list contains data for validation purposes as well as data to generate IST form all recommended IST algorithms subsequently, as well as uncertainty, quality levels and the alternative cloud mask from University of Leicester.

The final Felyx generated MUDB will collect and assemble the following information from any in situ IST observations available and from all SST observations from the Coriolis data archive (Pole wards of 50 North and South):

- SLSTR data from Eumetsat L1 (all RBT) and L2 (WCT and WST) either NTC or reprocessed data. Both Nadir view and oblige view data are required
  - all relevant channels for IST/SST and cloud screening
  - any relevant noise/quality data that are available and relevant
  - sun, satellite and view geometry
  - all SSTs from WCT and WST (including quality indicators and sun-satellite-view geometry)
  - NWP (25 layers from slstr data stream) for RTTOV processing (alternative to 60 layer from own NWP files (see **below))
- SLSTR IST recommended from WP 4 (will subsequently be calculated and added)
- Simulated observations
  - RTTOV simulated TOA TBs, using the 60(or 25 from L1b file) layer NWP information
- Cloud mask fields calculated from SLSTR products*
  - Native and cloud masks based on the official SLSTR cloud-over-ice ATBD [Liberti, G.L, 2017] Requirements are SLSTR level 1b, and surrounding 3x3 pixels in some cases
  - Alternative cloud-screening procedure developed at University of Leicester, based on SLSTR data and simulated TOA TBs (see section **Fejl! Henvisningskilde ikke fundet.**) [Ghent, D., 2017]. University of Leicester has approved the MUDB inventory list to be sufficient to produce the Leicester cloud mask.
- Daily sea-ice concentration (Operational product OSI-401-b)
- Metop IST (operational product OSI-205)
  - IST (‘surface_temperature’)
  - IST uncertainty (3 variables)
  - L2p_flags (ghrsst variable)
  - Processing_flags
  - Quality_level
  - Probability_of water
  - Probability_of_ice
  - View and sun geometry
- ECMWF NWP
  - Surface parameters : 2mT, Tsurf, wind speed 10m, cloud, total column water and water vapor, surface pressure

Validation of the products will be carried out over appropriate and representative areas and time periods relevant for the product coverage, as listed in section 4.1. A strategy for continuous validation is designed in the PVP.

5.2 In Situ data for validation

The most crucial requirements for the in-situ observations from section 4.1 are:

- Traceability of in situ observations
- Earth systems and observations should be sampled in a way that climate relevant changes can be resolved – i.e. diurnal, seasonal, inter-annual and long-term changes
- High priority for additional observations should be in focus in data-poor regions
- Min. 6 month data
- Representative in situ observations for the snow and ice surface temperatures.

In the general requirements (Chapter 4) it is discussed how the various requirements will be met in this work and where requirements are difficult to meet. It is particular difficult to comply with requirements of traceability and representativeness. From table 2, we see that the most common and traditional temperature observation platform in the Arctic (Drifting Buoy) has uncertainties up to 5 K. Moreover, these platforms are practically never retrieved for post calibration, thus making traceability impossible.

The table also indicates why radiometric surface temperature measurements are highly requested for satellite IST validation purposes, because their estimated uncertainty is less than 0.5 K. These data are sparse, but will be extensively applied in the validation work.

Traceable in situ observations is required, but practically not feasible for Arctic sea ice temperature observations. Most observation platforms break down and disappear, leaving no possibility of post calibration. Regarding AWS data with two or more temperature sensors, then it is possible to perform inter-comparison with other sensors, to check the sensor stability and to some extent to actually perform a post calibration.

The in-situ data for validation and MUDB are discussed in the PVP and in the MUDB inventory file.

Δx (km)	Δt (min)	Δz (m)	$\mu_{in\ situ}$ (°C)	$\mu_{\Delta x}$ (°C)	$\mu_{\Delta t}$ (°C)	$\mu_{\Delta z}$ (°C)	$\sqrt{\mu_{in\ situ}^2 + \mu_{\Delta x}^2 + \mu_{\Delta t}^2 + \mu_{\Delta z}^2}$ (°C)
1.0	10	IST_{skin}	0.2	0.12-0.25	0.34	0	0.41-0.47
1.0	30	IST_{skin}	0.2	0.12-0.25	0.71	0	0.75-0.78
1.0	60	IST_{skin}	0.2	0.12-0.25	1.11	0	1.13-1.16
1.0	10	T_{2m}	0.05	0.12-0.25	0.34	1.45 - 2.38	1.49-2.42
1.0	30	T_{2m}	0.05	0.12-0.25	0.71	1.45 - 2.38	1.62-2.50
1.0	60	T_{2m}	0.05	0.12-0.25	1.11	1.45 - 2.38	1.83-2.64
1.0	10	T_{buoy}	0.05	0.12-0.25	0.34	3.27 - 4.95	3.29-4.97
1.0	30	T_{buoy}	0.05	0.12-0.25	0.71	3.27 - 4.95	3.35-5.01
1.0	60	T_{buoy}	0.05	0.12-0.25	1.11	3.27 - 4.95	3.46-5.08

Table 2 Uncertainty budget for In-Situ measurements to represent skin temperature (from Høyer et al. 2018)

5.3 Input for production

The SLSTR IST prototype processor is illustrated in figure 7, showing the major processes inside the processor box area and all dynamical input data and output product in the small boxes outside the rectangle. Static filters, maps, look-up tables, like Probability Density Functions PDF's and fixed uncertainty tables are not shown.

Beside data input, a high performance RTM is also required for the SLSTR IST processor, as indicated in the figure.

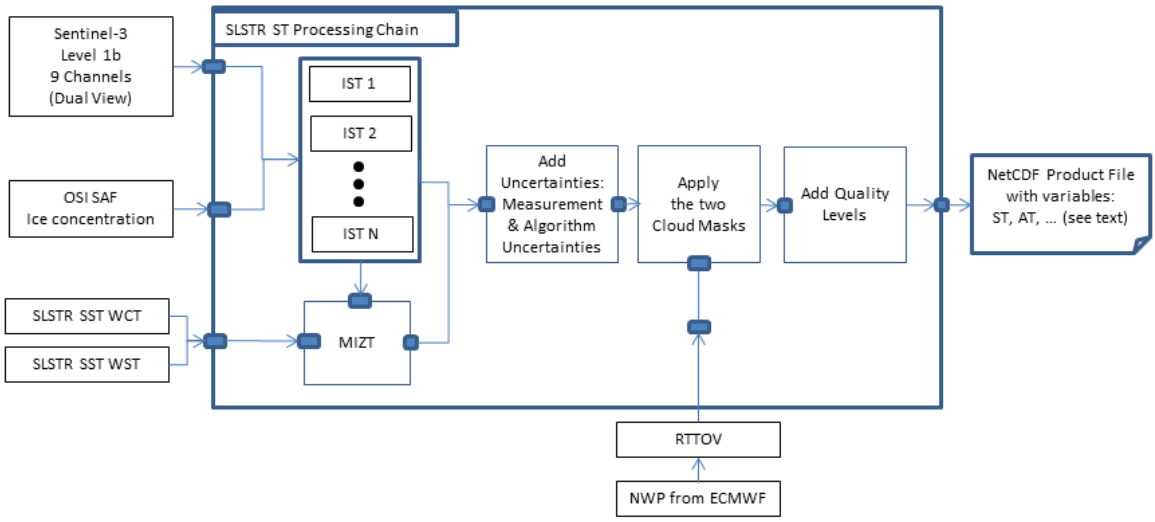

Figure 7: *The SLSTR IST processor dataflow. The processor uses three input data sources: Sentinel-3 SLSTR spectral channels, sea ice concentration and SST products (internal and recommended products), which allows the calculation of IST and MIZT. Subsequently, the uncertainty algorithms provide the distributed*

uncertainty estimates. Finally, clouded areas are masked, and the quality flag algorithm provides classification of the output data into different quality levels. The processor will allow switching between several IST algorithms (labelled in figure as IST1, …ISTN), five different SST data streams (WCT 1-4, WST), and two different cloud masks (C1, C2). The output product is saved in NetCDF format.

Following data are required for the SLSTR IST processor

- SLSTR data
  - All nine SLSTR channels in level 1b
  - Native cloud mask
  - Misc. quality indicators form input data
  - SST level-2 (WCT+WST)
- Cloud mask fields
  - The native SLSTR cloud products (Liberti et al.)
  - Alternative cloud-screening procedure developed at University of Leicester, based on SLSTR data and simulated TOA TBs (see section 5.5.6) (Ghent, D., 2017). Darren Ghent has approved the MUDB inventory list to be sufficient to produce the Leicester cloud mask (mail December 11)
- Daily sea-ice concentration (Operational product OSI-401-b)
- ECMWF NWP
  - Surface parameters : 2mT, Tsurf, wind speed 10m, cloud, total column water and water vapor, surface pressure
  - Atmospheric data (X Layers) : atmospheric profile of temperature, pressure and humidity
- A fast RTM for cloud mask processing and possibly for a bias correction scheme of the IST product.
- Static filters, maps and look-up tables

5.4 Product output

The development of a best possible IST product from SLSTR data will be carried out keeping in mind good praxis and principles from the product guidelines from the Global High Resolution Sea Surface Temperature (GHRSST) communities.

The GSOW requirements for product data format are provision in NetCDF format and compliancy to Climate and Forecast (CF-conventions, 2019) community standards. Additional nice-to-have requirements to the output data format are minimized file size and standardized data and attribute formats that are common to a wide range of users.

The Group for High Resolution SST (GHRSST) has for long been a mature component of the observing system and it has through comprehensive user surveys and under the supervision of a widely acknowledged science team, developed the L2P output format standard, described in the GHRSST Data Specification (GDS). The L2P format is widely applied by satellite and model communities. It complies with all above requirements, including compression of data with NetCDF4 technology that applies the HDF5 compression. Finally, the format is comprehensively documented and well defined (GDS v2).

It is recommended applying the L2P data format for SLSTR IST product output to the extent possible. Where the L2P standards do not apply for IST, we will use standards applied by the OSISAF IST product (Dybkjaer et al. 2018).

6 Requirement and Recommendation Summary

A summary of the requirements listed in Chapter 4 and 5 and the recommendations from the project team as discussed throughout the document and in the project proposal, is given here in Table 3. The summary table is organized with a requirement ID column, then the corresponding requirement type and the requirement it-selves. These columns are followed by the recommendation from the project team, a comment from project team, and a statement whether the recommendation is expected to lead to requirement compliancy. The last column indicates the origin of requirement.

Table 3 A list of identified product requirements from the GSOW, EO, climate, producer and user stakeholder groups. The table is also a compliancy matrix with requirement ID, requirement type (IO, Quality assessment, Processor, Product, Performance, and Algorithm), Requirement, and Recommendation (from project team),

Req. ID	Req. type	Requirement	Recommendation	Comment	Compliancy	Req. origin
R01	IO	Acceptable data format, e.g. L2P	Apply the L2P format described by GHRSST data format, GDS2.0. The GHRSST L2P format includes common standards from NetCDF and it is CF compatible.	The GDS is acknowledged by ocean data users and others.	Yes	MRTD, CLiC, , Copernicus/CMEMS
R02	Quality assessment	Operational validation	Prepare SLSTR IST processor for ongoing validation.	The PVP include recommendations for ongoing product validation and the validation will be done pixel wise, including quality level and uncertainty. This will be integrated in the	Yes	NRC

				prototype processor.		
R03	Quality assessment	Traceability of In Situ data	Separate validation into observation type. Set individual goals for each observation type.	Full traceability is not possible. However, sampling and observation uncertainties are estimated and will be subtracted from the performance assessment, depending of observation type.	No, but precautions taken	NRC, RTM, , Copernicus/CMEMS
R04	Quality assessment	Ensure data continuity from earlier IST products	Include other operational IST and NWP data in the diagnostic data set for at least 1 year.	A validation period of 1 year is chosen, including 1 year of OSISAF IST data for inter-comparison. IST from NWP is also included.	Yes	NRC,MRDT, , Copernicus/CMEMS
R05	Processor	Ensure generic programming code for IST processor	The processor will be coded in Python 3, including newest libraries.	Python is free software that is on the forefront of scientific programming and especially well-suited for satellite data analysis.	Yes	NRC, GSOW
R06	Processor	Reprocessing ready – ability to process large data sets	Make code modular and generic and hence flexible for both operation and reprocessing.	The code will not be made a dedicated code for reprocessing, but following good praxis will make it easily adaptable	Partly	NRC
R07	Product	Uncertainty – per pixel space and time dependent (K)	Develop a pixel wise, closed uncertainty budget.	An uncertainty algorithm for the SLSTR IST product is planned, based on the	Yes	CLiC, SOW, GSOW

				uncertainty algorithm from the OSISAF IST		
R08	Performance	SLSTR IST must have an accuracy (STD of differences) of 1 K at resolution of < 5 km (Goal 1 km)	Test a range of algorithms from simple 1 channel linear algorithms to dual channel and dual view channels with and without nonlinear angular corrections terms.	A range of algorithms are recommended for testing and the best algorithm(s) will be selected to represent various ice regimes. Copernicus (2018a) require 0.5 K in accuracy for IST. That is not realistic with current cloud screening techniques.	Probably not, but under positively clear sky conditions it is expected to get meet a 1.5 K requirement, at a pixel resolution (~1 km)	GSOW, RfOO, MRTD, GCOS, MRD (LST, including land ice), GMES MCS implementation plan, , Copernicus/CMEMS
R09	Performance	IST requirement is 1.0/1.3/2.0 K for 100/200/500 km grid for Goal/Breakthrough/Threshold, respectively.	Test a range of algorithms from simple 1 channel linear algorithms to dual channel and dual view channels with and without nonlinear angular corrections terms.	A range of algorithms are recommended for testing and the best algorithm(s) will be selected to represent various ice regimes. It is not possible to validate this requirement, because credible temperatures at 100-500 km grids are not available.	Probably	WMO rolling requirement review DB (OSCAR)
R10	Product	SLSTR IST product shall have a spatial resolution of 1-5 km (less priority than accuracy)	Produce SLSTR IST in FOV resolution, i.e. in swath projection.	Input and output projections are identical – level 1 in and level 2 out.	Yes	MRTD, Copernicus/CMEMS
R12	Product	Global coverage within 1-2 days (less priority than accuracy)	Apply all daily swath data	Even dual view swath width provides 100% coverage daily poleward of 50 North and South, or multiple	Yes	MRTD, GMES MCS implementation plan, Copernicus/CMEMS

				daily using only 1 satellite.		
R13	Algorithm	Use RTM tuning of algorithms in data sparse regions	The recommended algorithms will use RTTOV RTM model and ERA Interim atmospheric and surface data for model tuning	The ground data volume is small for ice surface both in the NH and in SH and all available data shall be used for validation and other diagnostics tasks.	Yes	RTM
R14	Product	Seamless interface across the MIZ	The MIZ temperatures are planned to be a function of IST and SST.	In the OSISAF IST the MIZT is the interpolated value between IST and IST – scaled by the radiative temperature in an appropriate range. The SLSTR MIZT will be inspired from that and thus ensuring seamlessness.	Yes	MRTD
R15	Product	Consider outcome of cloud screening	The SLSTR cloud screening product (from level 1) is compared with other cloud product over ice.	An inter-comparison between the native level 1 cloud screening product (Liberti et al.) and an alternative cloud screening product is planned in PVP	Yes	MRTD
R16	Product	Inter-calibration between successive sensors	Inter-calibrate Sentinel 3A with Sentinel 3B data in Product validation.	This is planned in the PVP document. A validation inter-comparison against OSISAF IST is also planned in the PVP	Yes	GMES Sentinel3 mission, GCOS
R17	Product/	Near real time production.	The SLSTR	Processor is planned to	Yes, probably	GMES MCS

	Processor		processor shall ingest NRT input data and therefor produce NRT output	work with NRT data, however, the production in depending of other SLSTR level 2 data (SST and cloud screening) which may delay production. The OSISAF IST timeliness is 3 hours, which probably also can be reached here. Copernicus (2018a) require a timeliness of 1 hour, which is less that the time of data availability for any production location.		implementation plan, Copernicus/CMEMS
R18	Quality assessment	High priority for additional observations shall be in focus in data sparse regions.	Collection of all available in situ data including land stations in the Arctic region.	All know in situ data are collected in the OSISAF in situ DB – and will be applied.	Yes (to our knowledge)	GCOS
R19	Product	Earth systems shall be sampled to enable analysis of diurnal, seasonal, inter-annual and long term changes	Level 2 production as recommended will mostly comply with R4+R10+R14 and hence with this requirement.	In situations where more frequent daily coverage is desired, then 2 SLSTR instruments can be applied	Yes	GCOS, Copernicus/CMEMS
R20	Quality assessment	Processing of diagnostic data sets shall be provided in NetCDF	Apply Felyx match up software	The Diagnostic data sets and validations will be done in Felyx software.	Yes	GSOW
R21	Algorithm	Algorithms to be implemented	Test the 6	The recommended	Yes	GSOW

		shall be either refinement to existing or newly developed alternative algorithms.	recommended algorithms described in chapter 3 (Equation SLSTR1 to SLSTR6)	algorithm range from simple and the state of the art split window and dual view algorithms that will be tested individually under different seasonal and geographical regimes		
R22	IO	Consolidate all input data, EO and ancillary data, required to produce SLSTR IT	All recommended data to produce SLSTR IST, generate cloud screening, perform validation and inter-comparison studies, are listed for approval.	The input data list in Chapter 5 is made in agreement with subcontractors that are responsible for algorithm calibration, additional cloud screening procedure and for generation of MUDB.	Yes	GSOW

6.1 Specific product characteristics and requirement for SLSTR IST

Following table is a list of the specific recommendations for the SLSTR IST output, based on requirements and discussions in chapters 4 and 5.

Table 4 Specific characteristics and product requirements for Sentinel-3 SLSTR IST output product.

IDENTIFICATION		
Product name	SLSR IST	
Satellite Input data	SLSTR L1b data stream (See IODD)	
Other input	SLSTR WCT/WST SST, OSISAF Ice Conc. (See IODD)	
Method	Multi Spectral Algorithm for skin temperature retrieval. (See ATBD)	
Dissemination means	EUMETCAST ? (TBD)	
Dissemination format	L2P, NetCDF	
Timeliness	NRT: 15 minutes processing time + time for level 1 availability at production centre.	
Spatial Coverage	Global: Pole wards of 50 N and 50 S.	
Spatial sampling	1 km	All processing is performed for the 1 km SLSTR grid
Projection	Swath	Adapted to 1 km SLSTR grid
Threshold accuracy	Bias=2.5 K STD= 3.0 K	Against high quality skin or air temperature measurements only See section 4.2.2
Target accuracy (Best realistic requirement)	Bias=1.5 K STD= 2.0 K	
Optimal accuracy	Bias=0.5 K STD= 0.8 K	
Data range	160 K - 300 K	
Verification method	Compared with radiometer or other high quality in situ data.	STD and mean error
Users	Met services, operational analysis and ocean model communities, research and climate studies and environmental studies.	

7 Acknowledgement

The European Union's Copernicus Programme funds this work.

8 References

Abbott, M.R et al. Issues in the Integration of Research and Operational Satellite Systems for Climate Research, Part II. Implementation – National Research Council, Division on Engineering and Physical Sciences, Commission on Physical Sciences, Mathematics, and Applications, Space Studies Board, Committee on Earth Studies, 2000.

Aoki, T. and 13 others. ADEOS-II/GLI snow/ice products — Part II: Validation results using GLI and MODIS data. Remote Sensing of Environment 111, 274-290, 2007.

Bjork, G. and Soderkvist, J.: Dependence of the Arctic Ocean ice thickness distribution on poleward energy flux in the atmosphere, J. Geophys. Res.-Oceans, 107, 3173, doi: 10.1029/2000JC000723, 2002.

CF-convensions. The conventions for Climate and Forecast (CF) metadata. http://cfconventions.org/, 2019.

CLiC. Observational needs for sea ice models - Short note. Discussion note from CLiC Arctic Sea Ice Working Group, http://www.climate-cryosphere.org/about, 2012.

CMEMS, 2016. BERTINO, L., L.A.BREIVIK, F.DINESSEN, Y.FAUGERE, G.GARRIC, B.HACKETT, J.A.JOHANNESSEN, T.LAVERGNE, P.-Y.LE TRAON, L.-T.PEDERSEN, P.RAMPAL, S.SANDVEN, H.SCHYBERG. Position paper Polar and snow cover applications User Requirements Workshop Brussels, COPERNICUS MARINE ENVIRONMENT MONITORING SERVICE MERCATOR OCEAN, VERSION 1, 23/06/2016-06-23.

CMEMS, 2017. CMEMS requirements for the evolution of the Copernicus Satellite Component. Copernicus Marine Environment Monitoring Service, Mercator Ocean and CMEMS partners, February 2017.

CMEMS, 2020. CMEMS Dashboard Upstream Satellite Data Requirements, V10.0 March 2020 (spreadsheet)Comiso, J.C., D.J. Cavalieri and T. Markus. Sea ice concentration, ice temperature, and snow depth using AMSR-E data. IEEE Transactions on Geoscience and Remote Sensing, 41, 2. doi: 10.1109/TGRS.2002.808317, 2003.

Copernicus 2018a. Duchossois, G., P. Strobl, V. Toumazou (Eds.) User Requirements for a Copernicus Polar Mission Phase 1 Report - User Requirements and Priorities. JRC Technical Report, doi:10.2760/22832, 2018.

Copernicus. 2018b. Duchossois, G., P. Strobl, V. Toumazou (Eds.) User Requirements for a Copernicus Polar Mission Phase 2 Report - High-level mission requirements. JRC Technical Report, doi:10.2760/44170, 2018.

Corlett, G.K., I.J.Barton, C.J.Donlon, M.C.Edwards, S.A.Good, L.A.Horrocks, D.T.Llewellyn-Jones, C.J.Merchant, P.J.Minnett, T.J.Nightingale, E.J.Noyes, A.G.O'Carroll, J.J.Remedios, I.S.Robinson, R.W.Saunders, J.G.Watts. The accuracy of SST retrievals from AATSR: An initial assessment through geophysical validation against in situ radiometers, buoys and other SST data sets. Advances in Space Research, Volume 37, Issue 4, Pages 764-769, 2006.

Dozier, J. and S. G. Warren. Effect of viewing angle on the infrared brightness temperature of snow. Water resources research 18(5), 1424-1434, 1982.

Donlon, C., B.Berruti, A.Buongiorno, M.-H.Ferreira, P.Féménias, J.Frerick, P.Goryl, U.Klein, H.Laur, C.Mavrocordatos, J.Nieke, H.Rebhan, B.Seitz, J.Stroede, R.Sciarra. The Global Monitoring for Environment and Security (GMES) Sentinel-3 mission. Remote Sensing of Environment, 120, pp 37-57, doi.org/10.1016/j.rse.2011.07.024, 2012.

Dybkjær, G., R. Tonboe, and J. L. Høyer: Arctic surface temperatures from Metop AVHRR compared to in situ ocean and land data. Ocean Sci., 8, 959–970, doi: 10.5194/os-8-959-2012.

Dybkjaer, G., S. Eastwood, A. L. Borg, and J. L. Høyer, R. Tonboe. OSI SAF Algorithm theoretical basis document for the OSI SAF High Latitude L2 Sea and Sea Ice Surface Temperature L2 processing chain. SAF/OSI/CDOP/DMI/SCI/MA/223, product OSI-205, Version 1.3, 2018.

GCOS: https://gcos.wmo.int/, 2019.

Ghent, D. and Sembhi, University of Leicester. Thermal Infrared Probabilistic Cloud Detection for Land Algorithm Theoretical Basis Document for Sentinel-3, S3-ATBD_UOL_CLOUDS_V3, 2017.

Ghent, D., Corlett, G., Goettsche, F., & Remedios, J. (2017) Global land surface temperature from the Along-Track Scanning Radiometers. Journal of Geophysical Research – Atmospheres, 122, 12167-12193, 2017B.

GHRSST Data Specification. GDS v2.0. https://www.ghrsst.org/about-ghrsst/governance-documents, 2012.

Haefliger, H., K Steffen and C Fowler. AVHRR surface temperature and narrow-band albedo comparison with ground measurements for the Greenland ice sheet. Annals of glaciology, 17, 1993.

Hall, D. K., G.A. Riggs, V.V. Salomonson. Algorithm Theoretical Basis Document (ATBD) for the MODIS Snow and Sea Ice-Mapping Algorithms. Earth Sciences Directorate NASA/Goddard Space Flight Center Greenbelt, MD 20771, 2001.

Hall, D. K., Williams, R. S., Steffen, K., and Chien, J. Y. L.: Analysis of Summer 2002 Melt Extent on the Greenland Ice Sheet using MODIS and SSM/I Data, Geoscience and Remote Sensing Symposium, 2004 IGARSS ’04 Proceedings, 2004 IEEE International, 5, 3029–3032, 2004a.

Hall, D. K., Key, J. R., Casey, K. A., Riggs, G. A., and Cavalieri, D. J.: Sea Ice Surface Temperature Product from MODIS, IEEE T. Geosci. Remote, 42, 1076–1087, 2004b.

Hall, D.K. and J.C. Comiso. A Satellite-Derived Climate-Quality Data Record of the Clear-Sky Surface Temperature of the Greenland Ice Sheet. Journal of Climate, https://doi.org/10.1175/JCLI-D-11-00365.1, 2012

Hall, D.K., J.C. Comiso, N.E. DiGirolamo, C.A. Shuman, J.E. Box, L.S. Koenig. Variability in the surface temperature and melt extent of the Greenland ice sheet from MODIS. Geophysical research letters, 40, 10, pp 2114-2120, doi.org/10.1002/grl.50240, 2013.

Høyer, J.L., A.M. Lang, R. Tonboe, S. Eastwood, W. Wimmer and G. Dybkjær. Report from Field Intercomparison Experiment (FICE) for ice surface temperature. Fiducial Reference Measurements for validation of Surface Temperature from Satellites (FRM4STS), ESA Contract No. 4000113848_15I-LG, 2017.

Høyer, J. L., E. Alerskans, P. Nielsen-Englyst , P. Thejll, G. Dybkjær and R. Tonboe, Detailed investigation of the uncertainty budget for Non-recoverable IST observations and their SI traceability, FRM4STS Technical Report, ESA Contract No. 4000113848_15I-LG, 2018.

Hori, M. T. Aoki, T. Tanikawa, H. Motoyoshi, A. Hachikubo, K. Sugiura, T. Yasunari, H. Eide, R. Storvold, Y. Nakajima, F. Takahashi. In situ measured spectral directional emissivity of snow and ice in the 8-14 microns atmospheric window. Remote Sensing of Environment, 100, 486-502, 2006.

Hori, M., T. Aoki, T. Tanikawa, A. Hachikubo, K. Sugiura, K Kuchiki and M. Niwano. Modelling angular-dependent spectral emissivity of snow and ice in the thermal infrared atmospheric window. Applied Optics, 52, 30, 2013.

Hultberg, T. and T. August. THE PIECEWISE LINEAR REGRESSION RETRIEVAL OF TEMPERATURE, HUMIDITY AND OZONE WITHIN THE EUMETSAT IASI L2 PPF VERSION 6. Internal EUMETSAT document: EUM/RSP/TEN/13/723383, 20xx.

Hutchison, K.D., R.L. Mahoney and B.D. Lisager. Discriminating sea ice from low-level water clouds in split-window, mid-wavelength IR imagery. Int. Journal of Remote Sensing, 34, 20, pp 7131-7144, 2013.

Hwang, B.J. and D. G. Barber. On the Impact of Ice Emissivity on Sea Ice Temperature. IEEE Geoscience and Remote Sensing Letters, 5, 3, 2008.

Hutchison, K.D., R.L. Mahoney and B.D. Lisager. Discriminating sea ice from low-level water clouds in split-window, mid-wavelength IR imagery. Int. Journal of Remote Sensing, 34, 20, pp 7131-7144, 2013.

Key, J. and Haefliger, M.: Arctic Ice Surface Temperature Retrieval from AVHRR Thermal Channels. J. Geophys. Res.-Oc. Atm., 97, pp 5885–5893, 1992.

Key, J.R., JB Collins, C Fowler, RS Stone. High-latitude surface temperature estimates from thermal satellite data. Remote Sensing of Environment, 61, 2, pp 302-309, 1997.

Key, J.R., R. Mahoney, Y. Liu, P. Romanov, M. Tschudi, I. Appel, J. Maslanik, D. Baldwin, X. Wang and P. Meade. Snow and ice products from Suomi NPP VIIRS. Journal of Geophysical Research: Atmospheres Volume 118, Issue 23, doi.org/10.1002/2013JD020459, 2013.

LaViolette, P. E.; Chabot, P. L. Nimbus II satellite sea surface temperatures versus historical data in a selected region: a comparative study. Deep-Sea Research and Oceanographic Abstracts, Volume 15, Issue 5, p. 617-622, 1968.

Liberti, G.L. Cloud screening over sea-ice and marginal ice zones: Final Report. Official SLSTR cloud mask for over ice, EUMETSAT/Copernicus, ITT No. 15/211424, 2017.

Lindsay, R.W. and D.A. Rothrock. Arctic sea ice temperature from AVHRR. Journal of Climate, 7, 1993.

Liu, Y., J. Key, M. Tschudi, R. Dworak, R. Mahoney and D. Baldwin. Validation of the Suomi NPP VIIRS Ice Surface Temperature Environmental Data Record. *Remote Sensing*, *7,* 12, pp 17258-17271; doi: 10.3390/rs71215880, 2015.

McMillin, L.M. Estimation of sea surface temperatures from two infrared window measurements with different absorption. Journal of Geophysical Research, 80, 36, 1975.

Marbouty, D. An experimental study of temperature gradient metamorphism. Journal of Glaciology 26(94), 303–312, 1980.

Merchant, C. SLSTR SST ATBD. SENTINEL-3 L2 PRODUCTS AND ALGORITHM DEFINITION. Sea surface temperature (SLSTR) Algorithm Theoretical Basis document. University of Edinburgh, Document Ref: SLSTR-ATBD-L2SST-v2.5, 2012.

MODIS-NASA MODIS Sea Ice and Ice Surface Temperature. https://modis.gsfc.nasa.gov/data/dataprod/mod29.php, 2018.

NOAA/NESDIS. https://ncc.nesdis.noaa.gov/VIIRS/, 2019.

Price, J.C. Land surface temperature from the split window channels of the NOAA 7 Advanced <very High Resolution Radiometer. J. of Geophys. Res., 89, D5, pp 7231-7237, 1984.

PROMICE Programme for Monitoring of the Greenland Ice Sheet. www.promice.org.

Rao, P.K., A. E. Strong, R. Koffler. Gulf Stream and Middle Atlantic Bight: Complex Thermal Structure as Seen from an Environmental Satellite. Science 06. Vol. 173, Issue 3996, pp. 529-530. doi: 10.1126/science.173.3996.529, 1971.

Rees, W. G., S. P. James. Angular variation of the infrared emissivity of ice and water surfaces. International Journals of Remote Sensing 13, 2873-2886, 1992.

Remedios, J. and S. Emsley. Land Surface Temperature, Sentinel-3 Optical Products and Algorithm Definition. Reference S3-L2-SD-03-T03-ULNILU-ATBD, Version 2.3, 2012.

Scambos, T. A., Haran, T. M., and Massom, R.: Validation of AVHRR and MODIS ice surface temperature products using in situ radiometers, Ann. Glaciol., 44, 345–351, 2006.

Stammer, D., Johanessen, J., LeTraon, P.-Y., Minnett, P., Roquet, H., and Srokosz, M.: Requirements for Ocean Observations Relevant to post-EPS, EUMETSAT Position Paper: AEG Ocean Topography and Ocean Imaging, 10 January 2007, version 3, 2007.

Steffen, K., Abdalati, W., and Stroeve, J.: Climate sensitivity studies of the Greenland ice sheet using satellite AVHRR, SSMR, SSM/I, and in situ data. Meteorol. Atmos. Phys., 51, 239–258, 1993.

Stroeve, J., M. Haefliger, and K. Steffen, 1996: Surface Temperature from ERS-1 ATSR Infrared Thermal Satellite Data in Polar Regions. J. Appl. Meteor., 35, 1231–1239, doi.org/10.1175/1520-0450(1996)035.

Stroeve, J. and Steffen, K.: Variability of AVHRR-Derived Clear-Sky Surface Temperature over the Greenland Ice Sheet, J. Appl. Meteorol., 37, 23–31, 1998.

Tonboe, R.T., G. Dybkjær, J.L. Høyer. Simulations of the snow covered sea ice surface temperature and microwave effective temperature. Tellus A 63 (5), 1028-1037, 2011.

USSP, United States Space Science Program. Report to COSPAR, Fifteenth meeting Madrid. National Academy of Science-National Research Council, Washington DC, 1972.

Veihelmann, B., Olesen, F. S., and Kottmeier, C.: Sea Ice surface temperature in the Weddell Sea (Antarctica), from drifting buoy and AVHRR data, Cold Reg. Sci. Technol., 33, 19–27, 2001.

Vincent, R. F., Marsden, R. F., Minnett, P. J., Creber, K. A.M., and Buckley, J. R.: Arctic waters and marginal ice zones: A composite Arctic sea surface temperature algorithm using satellite thermal data, J. Geophys. Res.-Oceans, 113, C04021, doi:10.1029/2007JC004353, 2008a.

Vincent, R.F., R. F. Marsden, P. J. Minnett and J. R. Buckley. Arctic waters and marginal ice zones: 2. An investigation of arctic atmospheric infrared absorption for advanced very high resolution radiometer sea surface temperature estimates. Journal of Geophysical Research, 113, C8, doi.org/10.1029/2007JC004354, 2008b.

Wan, Z., and J. Dozier. Land-surface temperature measurements from space: Physical principles and inverse modelling. IEEE Transactions on Geoscience and Remote Sensing, 27, 3, 1989.

Warren, S. G., and R. E. Brandt. Optical constants of ice from the ultraviolet to the microwave: A revised compilation, J. Geophys. Res., 113, D14220, doi: 10.1029/2007JD009744, 2008.

Wiebe, H. Implementation and validation of the snow grain size retrieval SGSP from spectral reflectances of the satellite sensor MODIS. PhD thesis, University of Bremen, 2011.

Wiscombe, W. J. and S. G. Warren. A model for the spectral albedo of snow. I: pure snow. Journal of the atmospheric sciences 37(12), 2712-2733, 1980.

Zavody, A.M., C.T. Mutlow and D.T. Llewellyn-Jones. A radiative transfer model for sea surface temperature retrieval for the along-track scanning radiometer. J. Geophys. Res., 100, No C1, pp 937-952, 1995.

Zhang, Z.M., B. K., Tsai, and G. Machin (eds.). Radiometric Temperature Measurements: I. Fundamentals, Academic Press/Elsevier, San Diego, 2009a.

Zhang, Z.M., B.K. Tsai and G. Machin (eds.). Radiometric Temperature Measurements: II. Applications. Academic Press, 18. nov. 2009. Remote Sensing of the earth's surface temperature, Chapter 6 Peter Minnett, 2009b.